

Stochastic field effects in a two-state system: symmetry breaking and symmetry restoring

Sara Oliver-Bonafoux,¹ Raúl Toral,¹ and Amitabha Chakrabarti²

¹*Instituto de Física Interdisciplinar y Sistemas Complejos IFISC (CSIC-UIB),
Campus UIB, 07122 Palma de Mallorca, Spain.*

²*Department of Physics, Kansas State University, Manhattan, KS 66506, USA.*

(Dated: December 23, 2024)

We propose a theoretical model that incorporates both a time-varying stochastic field and thermal noise in a two-state system. In analyzing data from numerical simulations, we adopt a detailed microscopic approach that goes beyond the standard calculation of the order parameter. Specifically, we measure the probability distribution of the magnetization as a function of temperature and field strength, and compute the time required for the system to jump from one ordered state to the other. These measurements enable us to probe various ordered states in the system and investigate the symmetry breaking and symmetry restoring phenomena underlying the observed phase behavior.

Introduction.—Acceleration of chemical reactions has been the focus of several recent studies [1]. The reaction rates for chemical reactions [2] and crystallization are often limited by mass transport or activation barriers [3]. In the context of electrodeposition, classical crystal growth and electrochemical crystallization, the introduction of stochastic electric fields has been shown to enhance ion heating and reaction rates [4, 5]. In such systems, particles experience stochastic forces due to thermal noise and an independent fluctuating electric field. Some experimental approaches apply a weakly fluctuating field, i.e., a bias field [6], in addition to a rapidly fluctuating field, and analyze the amplification of the effect of the weak bias field. This amplification is closely related to stochastic resonance phenomena [7].

Motivated by these experimental studies, we analyze a simple theoretical model that incorporates stochastic fields in addition to thermal noise in a two-state system. In our description of a system with a double-well potential and a barrier separating these minima, we choose the Ising model in a heat bath. The stochastic fields are implemented as random, time-varying, spatially homogeneous magnetic fields applied to the spins in the Ising model description. This allows us to study both the possibility of any non-equilibrium phase transition in the model along with how random fields facilitate barrier hopping in a two-state system. Even though the model studied by us is simple in its construction and has been looked into in the past albeit in a different context [8, 9], the richness of the phase diagram that we obtain is unprecedented. We believe that this model will illuminate theoretical foundations behind experimental studies mentioned before and will lead to additional experiments of barrier hopping in two-state systems in the presence of stochastic fields.

We find several effects associated with the presence of a time-varying magnetic field. First, it converts the usual symmetry-breaking phase transition of the Ising model into a noise-induced transition [10] between a soft-paramagnetic phase and

a soft-ferromagnetic phase. In the *soft* phases, the magnetization displays broad distributions around their maxima values, and their width and height remain finite in the limit of large size. Furthermore, the soft-ferromagnetic phase is characterized by a dynamical restoring of the symmetry between the two equivalent ferromagnetic states [11–13]. For small amplitude of the magnetic field, this transition occurs at the same critical temperature of the field-free Ising model. Second, at lower temperatures, a new transition appears between the soft-ferromagnetic phase and a *bona-fide* ferromagnetic phase where one of the two-equivalent ferromagnetic states is selected dynamically. This new transition is accompanied by a divergence of the characteristic time to jump between one ordered state and the other.

Model and simulation scheme.—Let us consider an Ising model in the presence of a time-varying, but spatially homogeneous, random magnetic field. The Hamiltonian of the system is

$$\mathcal{H} = -J \sum_{\langle i,j \rangle} s_i s_j - h(t) \sum_i s_i, \quad (1)$$

where $s_i \in \{-1, +1\}$ is the spin variable, $J > 0$ is the strength of the ferromagnetic exchange between nearest neighbours spins $\langle i, j \rangle$ and $h(t)$ is the time-dependent, but uniform in space, random magnetic field. We take $h(t)$ to be Gaussian distributed with zero mean and variance $2D$, where the parameter D sets the strength of the field. The $N = L \times L$ spins are distributed on a square lattice of side L with periodic boundary conditions.

Modeling the system in contact with an isothermal bath at temperature T , we introduce a heat bath stochastic dynamics with single spin random updates. After setting randomly the initial configuration, the evolution is such that a randomly chosen spin adopts a new value $s_i = \pm 1$, independent of the previous one, according to the probabilities

$$\begin{aligned} P(s_i = +1) &= (1 + e^{-2\beta b_i})^{-1}, \\ P(s_i = -1) &= 1 - P(s_i = +1), \end{aligned} \quad (2)$$

with $\beta = 1/(kT)$ and $b_i = J \sum_{\mu} s_{i_{\mu}} + h(t)$, where the sum over μ runs over the 4 nearest neighbours of the regular lattice. For simplicity, we set the Boltzmann constant, k , and the coupling constant, J , equal to 1 throughout the paper. Time t is measured in Monte Carlo steps (MCS), so that one unit of time corresponds to N spin updates. The random variable $h(t)$ remains constant during 1 MCS, after which a new random value $h(t+1)$ is selected independent of the previous one.

Probability distribution of magnetization.—In the following, we present the results obtained in numerical simulations in which, after a thermalization transient, we calculate the instantaneous magnetization,

$$m(t) = \frac{1}{N} \sum_{i=1}^N s_i, \quad (3)$$

at each MCS and determine its time-averaged stationary probability distribution, $P(m)$. We limit our analysis to moderate values of field strength D to allow for a balanced competition between phase ordering and stochastic effects. For large values of D ($\gtrsim 1$), we observe a very rich phenomenology (see Supplemental Material SM1) that we will not discuss in this paper.

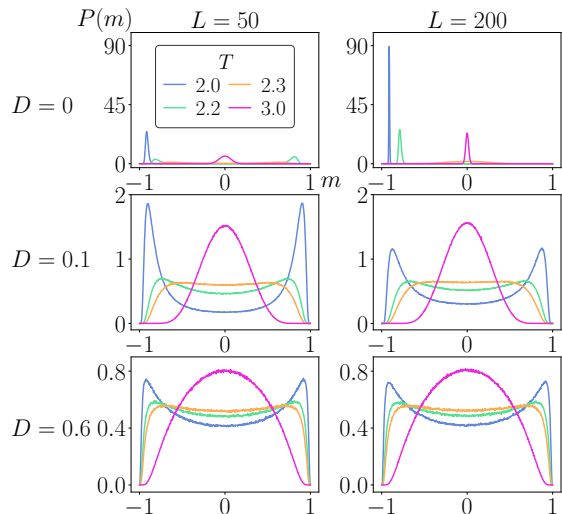


FIG. 1. Histograms of the normalized probability distribution $P(m)$ of the magnetization m for different field intensities ($D = 0, 0.1, 0.6$) for two system sizes ($L = 50, 200$) at several temperatures. Note that graphs in the same row have the same vertical scale. The results come from agent-based numerical simulations in which, after a thermalization period of 10^6 MCS, we have let the system evolve for 10^8 MCS and have measured the instantaneous magnetization every 10 MCS. Thus, the distributions $P(m)$ are derived from a sample of 10^7 measurements of m .

Fig. 1 shows the probability distribution of magnetization, $P(m)$, for three values of field strength D (including $D = 0$), at temperatures

close to the 2-d Ising equilibrium critical temperature, $T_c = 2.269$, and for two system sizes: $L = 50$ and $L = 200$. Let us first focus on the well-known Ising case, corresponding to $D = 0$. At temperatures below T_c , such as $T = 2.0$, the distribution exhibits a single peak at a non-zero magnetization value that gets sharper with increasing system size. At temperature $T = 2.2$, which is close to, but still below T_c , the distribution for the smallest system size ($L = 50$) shows two symmetric peaks close to $m \approx \pm 1$, indicating that the trajectories $m(t)$ are able to jump frequently between the two ordered states. These transitions, however, are absent for the largest system ($L = 200$). Above the critical temperature, the distribution exhibits a single peak at $m = 0$ that also becomes sharper as L increases. All these observations align with the expected behavior in the limit of infinite system size: a ferromagnetic phase, characterized by a symmetry-breaking Dirac-delta distribution centered in one of the two ordered states, for $T < T_c$; and a paramagnetic phase, characterized by a Dirac-delta distribution centered in the disordered state, for $T > T_c$.

Continuing the analysis of Fig. 1, we now focus on the results obtained for finite values of field strength D . We observe that, as temperature decreases, the system still undergoes a transition from a unimodal to a bimodal regime at the zero-field critical temperature T_c . However, the displayed behavior is significantly different from the $D = 0$ case. Notably, both for $D = 0.1$ and $D = 0.6$, at temperature $T = 2.0$ (below T_c), even for the largest system size ($L = 200$) the dynamical trajectories display jumps between the two ordered states. On the other hand, at temperature $T = 3.0$ (above T_c), the probability distribution for the largest system ($L = 200$) is still centered around $m = 0$, but is much wider than in the $D = 0$ scenario. Additionally, the $P(m)$ distributions show much less system size dependence compared to the field-free case, with even the smallest system ($L = 50$) exhibiting sharper distributions than the largest system ($L = 200$) at the same temperature. This result suggests that a wide distribution is obtained in the thermodynamic limit. Further evidence for this phenomenon and the unusual dependence on system size is provided in Supplemental Material SM2. Consequently, in the limit $L \rightarrow \infty$ we expect the following behavior: for $T \lesssim T_c$, a soft-ferromagnetic phase where the symmetry between the two ordered magnetization states is dynamically restored, leading to a probability distribution with two broad peaks centered around these states; and for $T > T_c$, a soft-paramagnetic phase characterized by a broad probability distribution around the disordered value of magnetization.

Fig. 2 shows the histograms of the probability distribution $P(m)$ for field intensities $D = 0.1$ and $D = 0.6$ at lower temperatures than those presented in Fig. 1. Let us first focus on the results

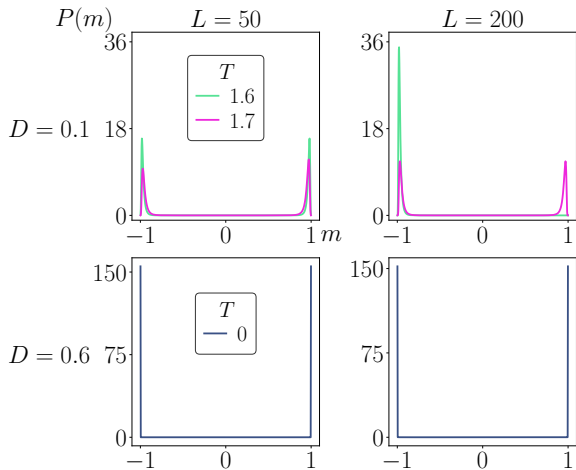


FIG. 2. Probability distribution $P(m)$ of the magnetization m for two system sizes ($L = 50, 200$) and for field intensities $D = 0.1$ and $D = 0.6$ at different temperatures. In the numerical simulations, the thermalization and measurement times have been set identical to those in Fig. 1.

obtained for $D = 0.1$. At temperature $T = 1.7$, the independence of the distributions with respect to system size, along with the observed dynamical restoring between the two ordered magnetization states, indicates that the system is in the soft-paramagnetic phase. In contrast, at a slightly lower temperature ($T = 1.6$), the behavior displayed resembles that of the field-free Ising model: the symmetry restoring phenomenon is a finite-size effect that is only exhibited by the smallest system ($L = 50$). These results suggest that at this temperature the system is in a *bona-fide* ferromagnetic phase. However, it is possible that with a longer observation time (beyond the 10^8 MCS considered in Fig. 2), a dynamical restoring between the two ordered magnetization states would be observed for all system sizes, indicating that the system might actually be in the soft-ferromagnetic phase. Therefore, what we can conclude is that for $D = 0.1$ and an observation time of 10^8 MCS, a transition between the soft-ferromagnetic and ferromagnetic phases occurs within the temperature range $1.6 < T < 1.7$. The nature of this transition and its dependence on observation time will be analyzed later. Let us now move to the results obtained for a field strength $D = 0.6$. In this case, due to the enhanced effects of the random magnetic field, the soft-ferromagnetic phase is exhibited even at temperature $T = 0$ and the ferromagnetic phase is not observed at any temperature.

Fig. 3 provides a comprehensive overview of the different phases exhibited in the model. The figure illustrates the maxima of the probability distribution of magnetization, m_{\max} , as a function of temperature for different field intensities, and for two system sizes. The Onsager's theoretical solution [14] for the field-free Ising model is also de-

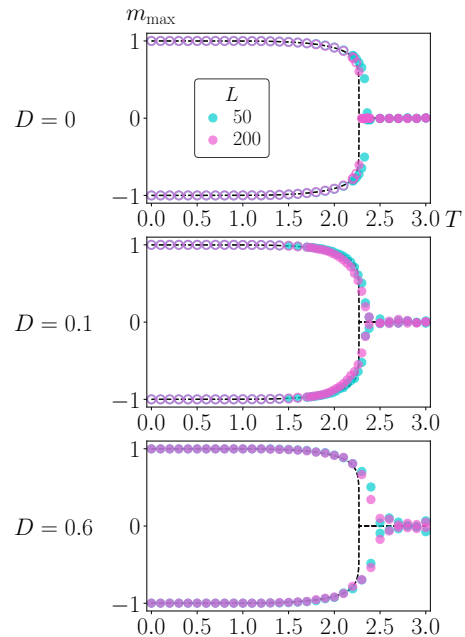


FIG. 3. Maxima m_{\max} of the probability distribution of magnetization, $P(m)$, as a function of temperature for several intensities of the random magnetic field ($D = 0, 0.1, 0.6$) and for two system sizes ($L = 50, 200$). The black dashed lines correspond to the Onsager's theoretical solution, while symbols represent the outcomes from numerical simulations. The same thermalization and measurement periods as in Fig. 1 have been applied here.

picted in the graphs. The three distinct phases that the system can exhibit are represented as follows: open circles located at two symmetric values, in the case of a ferromagnetic phase with symmetry breaking; colored circles, still symmetrically located, in the case of a soft-ferromagnetic phase with symmetry restoring; or colored circles around $m = 0$, in the case of a paramagnetic phase (including the soft case). For $D = 0$, the curve obtained for the largest system ($L = 200$) aligns more closely with Onsager's theoretical prediction than the curve corresponding to the smallest system ($L = 50$). Moreover, we observe that the exhibition of a soft-ferromagnetic phase is a finite-size effect that disappears as L increases. In the case of $D > 0$, on the other hand, the numerical curves also fit Onsager's theoretical prediction. Notably, for $D = 0.1$, even the results from the smallest system ($L = 50$) match more closely the theoretical curve than those from the largest system ($L = 200$). In the $D > 0$ scenario, unlike in the $D = 0$ case, the soft-ferromagnetic phase is exhibited, within a certain temperature range, for all system sizes. The temperature range in which the system is in the bimodal phase with symmetry restoring becomes larger as the field intensity increases. For the observation time considered in the figure (10^8 MCS), this temperature range cor-

responds to $1.6 \lesssim T \lesssim T_c$ for $D = 0.1$ and to $0 \leq T \lesssim T_c$ for $D = 0.6$. These results suggest that there is a critical value of the field strength, D_c , at which the ferromagnetic phase vanishes and the bimodal phase is always accompanied by a dynamical restoring of the symmetry between the two ordered states of magnetization.

Phase diagram and analysis of the transitions.—The numerical phase diagram of the model in the (D, T) plane is shown in Fig. 4, along with the characteristic shape of the probability distribution of the magnetization expected in the thermodynamic limit in the different regions of the diagram. It is well established that, in the field-free case, a symmetry-breaking phase transition occurs between the paramagnetic and ferromagnetic phases at the critical temperature T_c . Due to the addition of the random magnetic field, this phase transition transforms into a noise-induced transition [10], which is not accompanied by symmetry breaking in the thermodynamic limit. This transition, which occurs at the critical temperature T_c of the field-free model, separates the soft-paramagnetic and soft-ferromagnetic phases. On the other hand, the presence of the random field induces, at a temperature below T_c , a new phase transition between the soft-ferromagnetic phase and a ferromagnetic phase. This phase transition occurs at a temperature that decreases as the field strength increases, and disappears for field intensities $D > D_c \approx 0.6$.

In order to identify the boundary in the phase diagram separating the soft-ferromagnetic and ferromagnetic phases, we introduce a characteristic disordering time τ . We define this quantity arbitrarily, but precisely, as the average time the system takes to reach the disordered state $m = 0$ starting from the completely ordered state $m = -1$. In the soft-ferromagnetic phase, the system is able to jump from one ordered state to the other. Therefore, starting from the ordered state $m = -1$, we expect that after a finite time (even in an infinite system) the system will cross the barrier $m = 0$ on its way to the opposite ordered state, $m = +1$. In the ferromagnetic phase, in contrast, the system is not able to escape from an ordered state, resulting in a jump time that tends to infinity as system size increases. This new kind of phase transition between a soft-ferromagnetic and a ferromagnetic phase is therefore characterized by the divergence of the characteristic time τ . The colored lines in Fig. 4 separate, for a system of size $L = 100$, the region where the system can jump from $m = -1$ to $m = 0$ in a time less than τ_{\max} (which corresponds to the soft-ferromagnetic region), from the region in which the system is not able to make the transition (which corresponds to the ferromagnetic region). As the observation time τ_{\max} increases, the area of the ferromagnetic region decreases. Numerically, we cannot rule out the possibility that this region vanishes in the limit $\tau_{\max} \rightarrow \infty$, but we believe this is an unlikely scenario. Our results

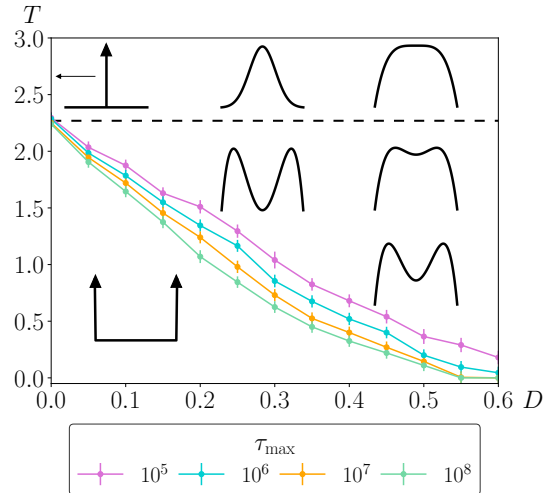


FIG. 4. Phase diagram in the (D, T) plane, showing the expected shape of the probability distribution of the magnetization in the thermodynamic limit in the different regions of the diagram. The horizontal dashed line indicates the critical temperature of the field-free Ising model, $T_c = 2.269$. The colored lines separating the soft-ferromagnetic and ferromagnetic phases come from numerical simulations for a system of size $L = 100$. In the simulations, given a value of D , we look for the first temperature at which the system is able to jump from $m = -1$ to $m = 0$ in a time shorter than a given observation time τ_{\max} . We then identify this temperature with the temperature of separation between the soft-ferromagnetic and ferromagnetic phases for that combination of D and τ_{\max} values. The curves shown in the figure are the result of repeating this operation 10 times and averaging the obtained results.

indicate that, for all practical purposes, the system exhibits both the soft-ferromagnetic and ferromagnetic phases. We note here that in experimental realizations of crystal growth phenomena, the time scale over which the field fluctuates (typically MHz frequency [6]) is much shorter than the typical observation time. Additionally, in Supplemental Material SM3, we include numerical results obtained in the mean-field description that support the results in two dimensions presented here.

The analysis of the average jump time introduced in this work proves to be a powerful method for inferring system properties. As detailed in Supplemental Material SM4, the calculation of this time enables the determination of the dynamic critical exponent, z , of the field-free Ising model, yielding results consistent with recent studies [15–17]. Consequently, we believe that the analysis of the jump time constitutes an effective technique for uncovering various system properties, including phase behavior and the corresponding phase diagram.

Conclusions.—In this paper we have analyzed a two-dimensional Ising model in the presence of a time-varying, but spatially homogeneous, Gaus-

sian random magnetic field. Although most of the existing works in the literature focus on the analysis of the time-averaged magnetization, we have shown that the distribution of magnetization, $P(m)$, provides valuable information about the phase behavior of the system. In particular, histograms of the magnetization are the key element for the identification of the soft-paramagnetic, soft-ferromagnetic and ferromagnetic phases in the model. The existence of a soft-ferromagnetic phase, a bimodal phase with symmetry restoring, has not been reported in previous studies that analyzed models similar to the one presented here. In [8], for instance, an Ising model with time-varying, but homogeneous in space, uniformly distributed random magnetic field is considered. The study is limited to the analysis of the averaged magnetization for a system of fixed size, so that

neither the presence of a bimodal phase with symmetry restoring nor its interesting dependence on system size is identified.

For future work, it would be valuable to consider an external magnetic field with an intrinsic correlation time, as this would better emulate real experimental conditions.

Acknowledgements.—Partial financial support has been received from Grant PID2021-122256NB-C21 funded by MICIU/AEI/10.13039/501100011033 and by “ERDF/EU”, and the María de Maeztu Program for units of Excellence in R&D, grant CEX2021-001164-M. S.O-B. acknowledges support from the Spanish Ministry of Education and Professional Training under the grant FPU21/04997. A.C. thanks Bret Flanders for many useful discussions.

-
- [1] Magdaléna Hromadová, Michal Valášek, Nicolangelo Fanelli, Hyacinthe N. Randriamahazaka, and Lubomír Pospíšil. Stochastic resonance in electron transfer oscillations of extended viologen. *The Journal of Physical Chemistry C*, 118:9066–9072, 5 2014.
- [2] Huan Wang, Myeonggon Park, Ruoyu Dong, Junyoung Kim, Yoon-Kyoung Cho, Tsvi Tlusty, and Steve Granick. Boosted molecular mobility during common chemical reactions. *Science*, 369(6503):537–541, 2020.
- [3] Krishna R Panta, Christine A Orme, and Bret N Flanders. Quantitatively controlled electrophoretic deposition of nanocrystal films from non-aqueous suspensions. *Journal of Colloid and Interface Science*, 636:363–377, 2023.
- [4] Ignacio A Martinez, Edgar Roldán, Juan MR Parrondo, and Dmitri Petrov. Effective heating to several thousand kelvins of an optically trapped sphere in a liquid. *Physical Review E—Statistical, Nonlinear, and Soft Matter Physics*, 87(3):032159, 2013.
- [5] Govind Paneru, Tsvi Tlusty, and Hyuk Kyu Pak. Bona fide stochastic resonance under nonGaussian active fluctuations. *Soft Matter*, 19(7):1356–1362, 2023.
- [6] B.F. Flanders. Private communication.
- [7] Luca Gammaitoni, Peter Hänggi, Peter Jung, and Fabio Marchesoni. Stochastic resonance. *Reviews of Modern Physics*, 70(1):223, 1998.
- [8] Mukdish Acharyya. Nonequilibrium phase transition in the kinetic Ising model: Dynamical symmetry breaking by randomly varying magnetic field. *Physical Review E - Statistical Physics, Plasmas, Fluids, and Related Interdisciplinary Topics*, 58:174–178, 7 1998.
- [9] Mukdish Acharyya. Nonequilibrium phase transitions in model ferromagnets: A review. *International Journal of Modern Physics C*, 16:1631–1670, 2005.
- [10] W Horsthemke and R Lefever. *Noise-Induced Transitions*. Springer, 1984.
- [11] C. Van den Broeck, JMR M. R. Parrondo, and R. Toral. Noise-induced nonequilibrium phase transition. *Physical Review Letters*, 73:3395, 12 1994.
- [12] C. Van den Broeck, JMR M. R. Parrondo, R. Toral, and R. Kawai. Nonequilibrium phase transitions induced by multiplicative noise. *Phys. Rev. E*, 55:4084, 4 1997.
- [13] R. Toral. Noise-induced transitions vs. noise-induced phase transitions. In *AIP Conference Proceedings*, volume 1332, pages 145–154, 2011.
- [14] R. J. Baxter. Onsager and Kaufman’s calculation of the spontaneous magnetization of the Ising model. *Journal of Statistical Physics*, 145(3):518–548, 2011.
- [15] M. P. Nightingale and H. W. J. Blöte. Monte Carlo computation of correlation times of independent relaxation modes at criticality. *Phys. Rev. B*, 62:1089–1101, Jul 2000.
- [16] Charlie Duclut and Bertrand Delamotte. Frequency regulators for the nonperturbative renormalization group: A general study and the model A as a benchmark. *Phys. Rev. E*, 95:012107, Jan 2017.
- [17] L.Ts. Adzhemyan, D.A. Evdokimov, M. Hnatič, E.V. Ivanova, M.V. Kompaniets, A. Kudlis, and D.V. Zakharov. The dynamic critical exponent z for 2d and 3d Ising models from five-loop ϵ expansion. *Physics Letters A*, 425:127870, 2022.
- [18] Kerson Huang. *Statistical mechanics*. John Wiley & Sons, 2008.

Supplemental Material

SM1. BEHAVIOR OBSERVED FOR LARGE VALUES OF FIELD STRENGTH

In this section, we briefly present the intriguing behavior displayed for high values of the random magnetic field strength, D . Fig. SM1 shows the histograms of the probability distribution of magnetization, $P(m)$, obtained for large values of field intensity at two different temperatures, T . As the field strength increases, the histograms reveal peaks that are absent for moderate noise intensities ($D < 1$). A detailed analysis of the complex phenomenology observed here will be addressed in future work.

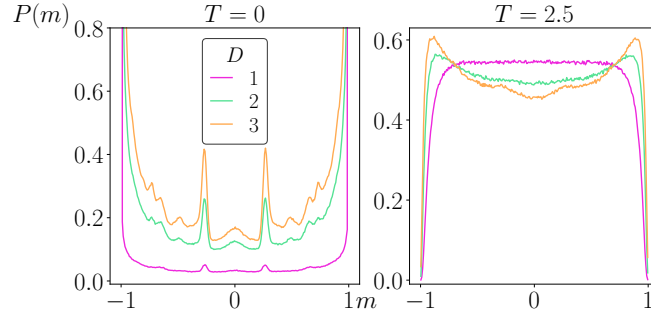


FIG. SM1. Histograms of the normalized probability distribution $P(m)$ of magnetization m for different values of noise intensity ($D = 1, 2, 3$) at two different temperatures ($T = 0, 2.5$) for a system size $L = 32$. The results have been obtained in numerical simulations in which, after a thermalization period of 10^6 MCS, we have taken 10^7 measurements of the instantaneous magnetization leaving 10 MCS between consecutive measurements.

SM2. EXISTENCE OF A WIDE LIMITING DISTRIBUTION IN THE SOFT-FERROMAGNETIC PHASE

Fig. SM2 shows the probability distribution of magnetization, $P(m)$, for two values of noise intensity ($D = 0.1, 0.6$) and for several system sizes ($L = 50, 100, 300, 500$) at a fixed temperature. For each noise intensity, the corresponding temperature lies, according to the phase diagram in Fig. 4, within the soft-ferromagnetic phase, which is characterized by a dynamical restoring of the symmetry between the two ordered states of magnetization. We first note the unusual dependence of the probability distribution on system size, which becomes wider as system size increases. Additionally, the distributions for the larger system sizes ($L = 300, 500$) for fixed D and T completely overlap, indicating that a limiting wide distribution is reached as system size increases.

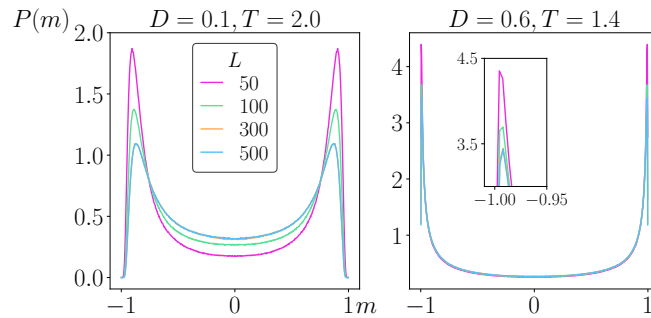


FIG. SM2. Probability distribution of magnetization, $P(m)$, for several system sizes and for $D = 0.1$ and $T = 2.0$ (left panel), and for $D = 0.6$ and $T = 1.4$ (right panel). In the numerical simulations, we have taken 10^7 measurements of the instantaneous magnetization after an initial transient of 10^6 MCS.

SM3. MEAN-FIELD DESCRIPTION

In this section, we present several numerical results obtained in the mean-field description of the model. As in the main text, we set the coupling constant, J , and the Boltzmann constant, k , equal to 1.

In the two-dimensional agent-based model, the system evolves through single spin updates in which a randomly chosen spin adopts a new state $s_i = \pm 1$, independent of the previous one. The probability that the new value is $s_i = +1$ is

$$P_i^+ \equiv P(s_i = +1) = \left[1 + e^{-\frac{2}{T}(\sum_{\mu} s_{i_{\mu}} + h(t))} \right]^{-1}, \quad (\text{SM1})$$

where the sum over μ runs over the 4 nearest neighbours of the regular lattice. We recall that the magnetic field $h(t)$ is spatially homogeneous, but varies in time. Specifically, at each MCS, a random value for $h(t)$ is sampled from a Gaussian distribution of zero mean and variance $2D$.

In the mean-field description, the probability in Eq. (SM1) is approximated as

$$P_i^+ \approx \left[1 + e^{-\frac{2}{T}(4m(t) + h(t))} \right]^{-1}. \quad (\text{SM2})$$

After the update of spin i , i.e., after a time $\Delta t = 1/N$, the three possible values for $m(t + \Delta t)$ are: $m(t) + 2/N$ (spin i has flipped from -1 to $+1$), $m(t) - 2/N$ (spin i has flipped from $+1$ to -1), and $m(t)$ (spin i has not changed its state). Denoting the probability $P[m(t + \Delta t) = m' | m(t) = m]$ as $P(m \rightarrow m')$, the probabilities associated with these three possible outcomes can be written as:

$$\begin{aligned} P\left(m \rightarrow m + \frac{2}{N}\right) &= \frac{1 - m}{2} \cdot P_i^+, \\ P\left(m \rightarrow m - \frac{2}{N}\right) &= \frac{1 + m}{2} \cdot (1 - P_i^+), \\ P(m \rightarrow m) &= 1 - P\left(m \rightarrow m + \frac{2}{N}\right) - P\left(m \rightarrow m - \frac{2}{N}\right), \end{aligned} \quad (\text{SM3})$$

where we have used that the fraction of spins in state $+1$ and -1 are $\frac{1+m}{2}$ and $\frac{1-m}{2}$, respectively. Starting from an initial flat distribution, $P(m, t = 0)$, we use these transition probabilities to find $P(m, t + \Delta t)$ from $P(m, t)$ iteratively and compute the steady-state values after a thermalization transient.

A. Probability distribution of magnetization

In Fig. SM3, we show the numerical probability distribution of the magnetization, $P(m)$, obtained in the mean-field description for two noise intensities ($D = 0, 0.1$) at several temperatures, and for two system sizes. First, we note that the critical temperature of the two-dimensional Ising model, $T_c = 2.269$, shifts to $T_c^{\text{MF}} = 4$ in the mean-field theoretical framework. This result, well-established in the field-free case [18], also holds for noise intensities $D > 0$. The behaviour displayed in the mean-field description is analogous to that observed in two dimensions. For $D = 0$, the system undergoes a phase transition between a paramagnetic and a ferromagnetic phase at temperature T_c^{MF} . Due to the addition of the magnetic field, this phase transition becomes a noise-induced transition between a soft-paramagnetic and a soft-ferromagnetic phase. Both phases are characterized by broad magnetization distributions centered around their maxima values, with both width and height remaining finite in the limit of large size.

Fig. SM4 shows the histograms of the magnetization for a field strength $D = 0.1$ at temperature $T = 0.5$, which is lower than those considered in Fig. SM3. At this temperature, the system is in the ferromagnetic phase and exhibits probability distributions centered around an ordered state of the magnetization that become sharper as the system size increases. This result indicates that, in the mean-field description for a field strength $D > 0$, the system undergoes a transition from a soft-ferromagnetic to a ferromagnetic phase at a temperature $T < T_c^{\text{MF}}$, as in the two-dimensional agent-based problem.

B. Boundary in the phase diagram separating the soft-ferromagnetic and ferromagnetic phases

In Fig. SM5, we show the boundary in the (D, T) plane separating the soft-ferromagnetic and ferromagnetic phases for different values of the observation time τ_{max} . As in the two-dimensional case, the

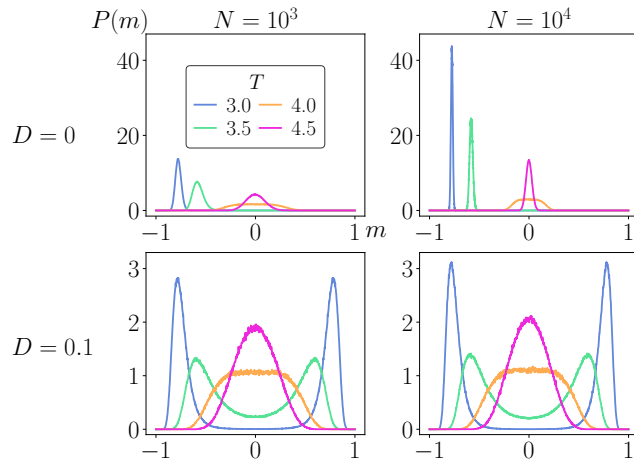


FIG. SM3. In the mean-field description, histograms of the normalized probability distribution of the magnetization, $P(m)$, for two system sizes ($N = 10^3, 10^4$) and for two noise intensities ($D = 0, 0.1$) at several temperatures. We have started the numerical simulations at the initial condition $m = 0$ and let the magnetization evolve according to the transition probabilities in Eqs. (SM3). After a thermalization transient of 10^5 MCS, we have taken measures of the instantaneous magnetization during an additional period of 10^6 MCS.

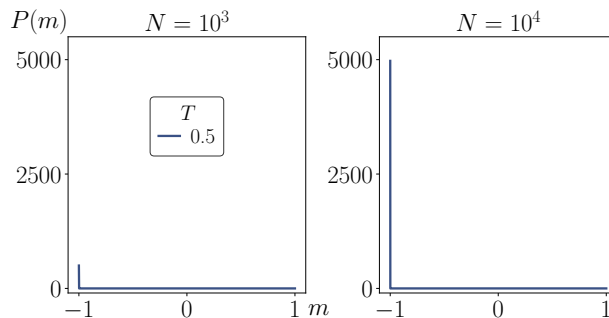


FIG. SM4. In the mean-field description, probability distribution of the magnetization for a field intensity $D = 0.1$ at temperature $T = 0.5$, and for two system sizes ($N = 10^3, 10^4$). Note that the two graphs have the same vertical scale. In the numerical simulations, we have set the same initial condition and the same thermalization and measurement periods as in Fig. SM3.

separation lines between the two phases have been obtained by identifying the temperature at which the jump time τ is greater than the observation time. The results obtained in the mean-field description are consistent with those of the two-dimensional case shown in Fig. 4.

SM4. DETERMINATION OF THE DYNAMIC CRITICAL EXPONENT IN THE FIELD-FREE ISING MODEL BY MEANS OF THE JUMP TIME

In a second-order phase transition, at the critical point, the correlation time τ scales with the system size L as

$$\tau \sim L^z, \quad (\text{SM4})$$

where z is the dynamic critical exponent.

In this section, we show that the average jump time τ the system takes to reach the disordered state $m = 0$ starting from the initial ordered state $m = -1$ can be used to compute the z exponent of the field-free Ising model ($D = 0$). Fig. SM4 shows the dependence of the average jump time τ on system size L at the critical temperature $T_c = 2.269$ in the field-free case. Fitting the data to Eq. (SM4) gives a value of the dynamic critical exponent of $z = 2.178(3)$. This result is not far from the value $z = 2.14(2)$ obtained recently in [17] using a five-loop ε expansion.

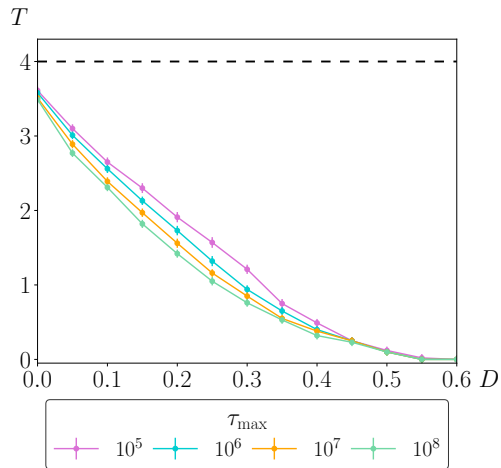


FIG. SM5. Separation line between the soft-ferromagnetic and ferromagnetic phases in the (D, T) plane obtained in the mean-field description for several observation times τ_{\max} . The horizontal dashed line indicates the critical temperature of the field-free Ising model in the mean-field description, $T_c^{\text{MF}} = 4$. The numerical scheme implemented to obtain the curves is identical to that used in the two-dimensional agent-based problem (see Fig. 4).

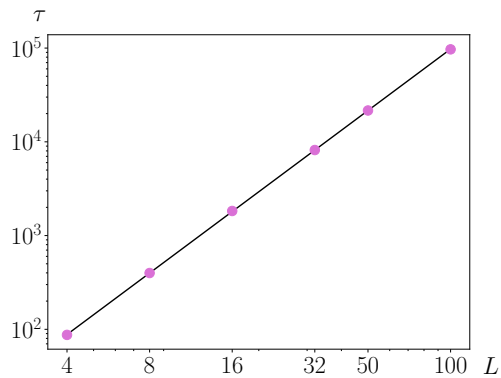


FIG. SM6. Average jump time τ versus system size L in the field-free Ising model ($D = 0$) at the critical temperature T_c . The jump times have been averaged over 10^4 realizations. The solid line represents the fit of the data to Eq. (SM4). The error bars are smaller than the symbol size and are therefore not visible.